



ARL-TR-7322 • JUNE 2015



Visualization and Measurement of the Deflagration of Metal-Foil Bounded JA2

John J Ritter and Anthony Canami

Approved for public release; distribution is unlimited.

NOTICES

Disclaimers

The findings in this report are not to be construed as an official Department of the Army position unless so designated by other authorized documents.

Citation of manufacturer's or trade names does not constitute an official endorsement or approval of the use thereof.

Destroy this report when it is no longer needed. Do not return it to the originator.



Visualization and Measurement of the Deflagration of Metal-Foil Bounded JA2

John J Ritter and Anthony Canami

Weapons and Materials Research Directorate, ARL

REPORT DOCUMENTATION PAGE				Form Approved OMB No. 0704-0188	
<p>Public reporting burden for this collection of information is estimated to average 1 hour per response, including the time for reviewing instructions, searching existing data sources, gathering and maintaining the data needed, and completing and reviewing the collection information. Send comments regarding this burden estimate or any other aspect of this collection of information, including suggestions for reducing the burden, to Department of Defense, Washington Headquarters Services, Directorate for Information Operations and Reports (0704-0188), 1215 Jefferson Davis Highway, Suite 1204, Arlington, VA 22202-4302. Respondents should be aware that notwithstanding any other provision of law, no person shall be subject to any penalty for failing to comply with a collection of information if it does not display a currently valid OMB control number.</p> <p>PLEASE DO NOT RETURN YOUR FORM TO THE ABOVE ADDRESS.</p>					
1. REPORT DATE (DD-MM-YYYY) June 2015		2. REPORT TYPE Final		3. DATES COVERED (From - To) 1 Sept 2014–28 Feb 2015	
4. TITLE AND SUBTITLE Visualization and Measurement of the Deflagration of Metal-Foil Bounded JA2				5a. CONTRACT NUMBER	
				5b. GRANT NUMBER	
				5c. PROGRAM ELEMENT NUMBER	
6. AUTHOR(S) John J Ritter and Anthony Canami				5d. PROJECT NUMBER	
				5e. TASK NUMBER	
				5f. WORK UNIT NUMBER	
7. PERFORMING ORGANIZATION NAME(S) AND ADDRESS(ES) US Army Research Laboratory ATTN: RDRL-WML-D Aberdeen Proving Ground, MD 21005-5066				8. PERFORMING ORGANIZATION REPORT NUMBER ARL-TR-7322	
9. SPONSORING/MONITORING AGENCY NAME(S) AND ADDRESS(ES)				10. SPONSOR/MONITOR'S ACRONYM(S)	
				11. SPONSOR/MONITOR'S REPORT NUMBER(S)	
12. DISTRIBUTION/AVAILABILITY STATEMENT Approved for public release; distribution is unlimited.					
13. SUPPLEMENTARY NOTES					
14. ABSTRACT The US Army Research Laboratory conducted experiments to broaden its knowledge of the mechanisms underlying the deflagration of nitrate ester-based propellants embedded with thermally conductive components. JA2 was employed for the experiments. Strands were bonded on 1 side with 0.001-inch-thick aluminum foil, and their deflagration was videographically recorded. The data yielded measured values for 1) the JA2 stock's normal linear burning rate, 2) test article burning rates relative to an axis parallel to their side wall, and 3) the angle between the burning surface and the side wall. The condensed-phase to gas-phase mass conversion rates for foil-bounded sections were 1.5–2.5 times higher than those for foil-less sections. The increases appear to be almost entirely due to increases in the area of the burning surface rather than an increase in the normal linear burning rate. It was also found that the pressure dependence of the gas generation rates for foil-bounded sections was slightly less than that for foil-less sections. Finally, the videographs clearly showed that the gas-phase flame has cellular structure. Because the test articles have relatively simple geometry, the results produced provide a good basis with which to validate computational fluid dynamics models for simulating the deflagration of wire-embedded propellants.					
15. SUBJECT TERMS JA2, enhanced burning rate, foil-embedded propellant, strand burner					
16. SECURITY CLASSIFICATION OF:			17. LIMITATION OF ABSTRACT UU	18. NUMBER OF PAGES 32	19a. NAME OF RESPONSIBLE PERSON John J Ritter
a. REPORT Unclassified	b. ABSTRACT Unclassified	c. THIS PAGE Unclassified			19b. TELEPHONE NUMBER (Include area code) 410-278-6180

Contents

List of Figures	iv
List of Tables	iv
Acknowledgments	v
1. Introduction	1
2. Experimental Methods	2
2.1 Test Article Fabrication	2
2.2 Measurement Techniques	3
3. Results	4
3.1 Configuration No. 1	4
3.2 Configuration No. 2	8
3.3 Other Observations	14
4. Summary and Conclusions	14
5. References	16
Appendix. Raw Data	17
List of Symbols, Abbreviations, and Acronyms	23
Distribution List	24

List of Figures

Fig. 1	Images of JA2 configurations used for experiments and modeling: a) modeled configuration, b) experimental configuration no. 1, and c) experimental configuration no. 2	3
Fig. 2	Schematic of strand burner facility (left), windowed strand burner (middle), and control panel (right).....	4
Fig. 3	Results obtained with configuration no. 1 test article: 1) foil-less section (left), 2) section with 0.001-inch-thick Al foil attached to right side (right).....	5
Fig. 4	Data obtained with a configuration no. 1 test article	5
Fig. 5	Bimodal burning rate enhancement of JA2 with foil. (The burning rate of foil-less sections at this pressure were found to be approximately 1.05 cm/sec.)	7
Fig. 6	Consecutive images from JA2 foil experiment at 3.48 MPa. The foil placed on the right side of the propellant for heat transfer purposes is circled. Note the right image has side ignition.	8
Fig. 7	Test article.....	9
Fig. 8	Image of article burning at 3.52 MPa	9
Fig. 9	Test 2, 6.94 MPa burning rate data. Blue is foil-less JA2, red is foil-bounded.....	10
Fig. 10	Test 8, 2.05 MPa burning rate data. Blue is foil-less JA2, red is foil-bounded.....	11
Fig. 11	Summary of burning rate vs. pressure for neat and foiled JA2	12
Fig. 12	Diagram of deflagration profile	13
Fig. 13	Close-up of burning surface illustrating cellular flame structure	14

List of Tables

Table 1	Initial foiled JA2 burning rate data	6
Table 2	Foiled JA2 burning rate data.....	11

Acknowledgments

This research effort could not have been possible without contributions from Dr Michael McQuaid, Dr Michael Nusca, and Mr Zachary Wingard.

INTENTIONALLY LEFT BLANK.

1. Introduction

The US Army Research Laboratory (ARL) in collaboration with the US Army Missile Research, Development, and Engineering Center (AMRDEC) is seeking approaches to enhance the gas-generation rates of minimum smoke rocket propellant formulations without increasing their vulnerability to external threats. One approach is to embed them with thermally conductive wires. By enabling localized conductive heat transfer from the combustion zone into the uncombusted propellant,¹⁻⁶ the wires serve as an ignition source that creates conically shaped burning surfaces. Reported as early as 1955⁷ and fielded in the 1960's (Redeye, Stinger missile systems), this approach has not become a standard because it is difficult and costly to implement reliably. Two significant challenges include casting the propellant grains without breaking the wires and properly bonding the propellant material to the wires such that there are no voids.

Given the challenges of reliably manufacturing wire-embedded propellant grains, performance increases need to be significant to justify an attempt to field the technology. However, the limited understanding of the phenomenon that exists today makes it hard to realize the technology's full potential. Only empirical models of the process have been developed to date; and they have not proven useful as design tools. Design parameters include the wires' thermophysical properties and diameter(s), their number, spacing and orientation within the grain, and the thermophysical and chemical kinetics properties of the propellant formulation. As a result, AMRDEC has had to rely on experimental (trial and error) testing of various wire-propellant combinations as a basis for developing motor designs.

Seeking to address this issue, ARL is developing a state-of-the-art computational fluid dynamics (CFD) model for simulating the phenomenon.^{8,9} As part of the effort, ARL is seeking experimental data that can be employed for model validation. In particular, direct observation of burning surfaces produced by various configurations of propellant and thermally conductive material is desired. Results from prior experiments with wire-embedded JA2 were previously published.⁵ Unfortunately, the fine-grid spacings required to model strands embedded with thin (0.002 to 0.010 mil) Ag wires made it too computationally expensive to attempt to model them. Therefore, strands embedded with foils of like thickness were modeled instead. Because the modeled configurations involved much larger contact areas, and therefore much higher heat transfer rates, they produced much larger gas phase generations rates. While certainly consistent with expectations, the comparisons were not considered to provide the level of validation that was desired.

To produce results that could be directly compared to a system that was practical to model, a new set of experiments were conducted. In them, JA2 strands were configured with a 0.001-inch-thick aluminum foil bounding 1 side. Significant differences between the results obtained with such configurations and those obtained with wire-embedded strands were observed. The findings are discussed.

2. Experimental Methods

2.1 Test Article Fabrication

The propellant chosen for these experiments was JA2. This was done for several reasons:

- JA2 is composed of nitrocellulose (NC), nitroglycerin (NG), and diethylene glycol dinitrate (DEGDN). As such, it is chemically similar to minimum smoke rocket propellants.
- ARL has developed a model with detailed gas phase chemical kinetics that accurately reproduces the burning rate of JA2.^{10,11}
- JA2 stock was readily available for use in preparing test articles.

Similar to the previous experiments, symmetry considerations led to a simplification in test article design. That is, instead of sandwiching a foil between 2 JA2 sheets—which proved difficult to implement reliably—articles were made by bounding only 1 side of 1 sheet, creating a half sandwich. Figure 1 shows configurations that were built and compares them to the modeled configuration. Green represents the JA2 sheet and the gray represents the thermally conductive material.

The JA2 strands were prepared from 0.150-inch-thick sheet stock. Strands had a nominal width of 0.5 inch and a height of 2.0 inch (Figs. 1b and 1c). To them, a 0.001-inch-thick aluminum foil was bonded to 1 side with Elmer's school glue. (The presence of the glue did not appear to impact the results.) Strands employed during the early stages of this study were built with the foil covering its entire height. Later, it only covered the bottom half. This configuration permitted burning rates for foil-less and foil-bounded sections to be acquired in 1 test. We also note that as long as the strand had smooth surfaces, particularly where it was cut, it was not necessary to use an inhibitor because edge effects did not present themselves.

For the first set of experiments, the foil was placed on the wider (0.5 inch) face. However, the results obtained with this configuration (no. 1) proved to be erratic. Therefore, a second set of experiments was conducted in which the foil was bonded

to the 0.150-inch-wide face (Fig. 1c). Results obtained with this configuration (no. 2) proved to be more reproducible, and most of our conclusions are drawn from those results.

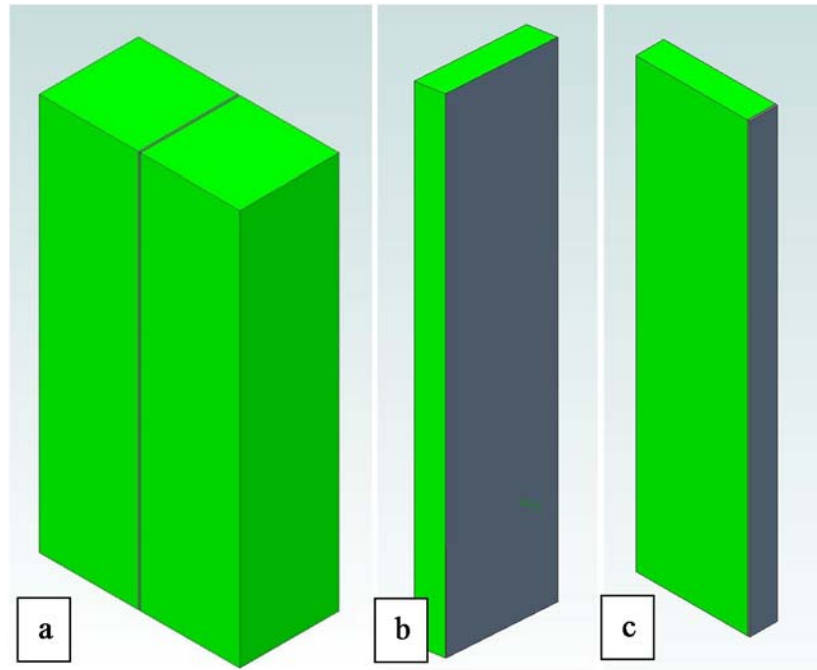


Fig. 1 Images of JA2 configurations used for experiments and modeling: a) modeled configuration, b) experimental configuration no. 1, and c) experimental configuration no. 2

2.2 Measurement Techniques

All experiments were conducted in the ARL's low-pressure strand burner (Fig. 2).¹² The apparatus includes a windowed chamber that is capable of being pressurized to 10 MPa (1,450 psi). Nitrogen was employed as the bath gas. To maintain constant pressure, the system includes a ballast tank that adds considerably to the system's overall volume, thus negating pressure increases due to propellant combustion. Pressure was measured with both a Setra Systems pressure transducer and a Heise mechanical dial gauge. The desired chamber pressure for each experiment was established just prior to ignition. Ignition was achieved by electrically heating a nichrome wire placed on top of the strand. Events were recorded with a Phantom high-speed camera equipped with a fixed 50-mm Nikon lens and an aperture setting of f/16. Images were acquired at 60 fps with exposure ranging from 3 to 10 μ s. To prevent smoke and soot buildup from obscuring the camera's view, a slow, steady stream of nitrogen was flowed through the chamber over the course of each experiment. Gas flowed from the inlet at the center of the chamber base toward the exhaust port located at the center top of the chamber.

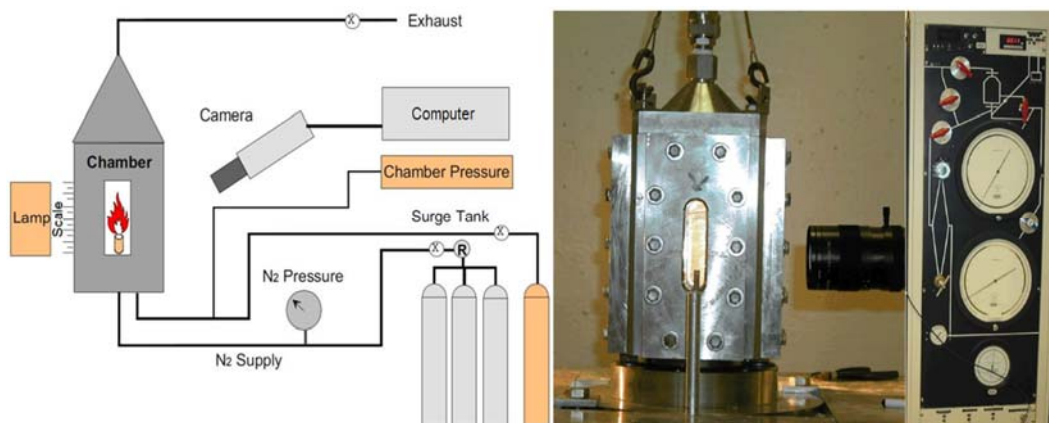


Fig. 2 Schematic of strand burner facility (left), windowed strand burner (middle), and control panel (right)

The test articles were burned at a constant pressure in the range 2.00–6.98 MPa (290–1,010 psi). To obtain burning rates, the flame propagation was measured as a function of time along the strands' foil-bonded edge. Linear least squares fits to the data yielded the reported burning rates.

3. Results

3.1 Configuration No. 1

Foil-less sections of JA2 strands burned in cigarette-like fashion and burning rates were easily measured. Once the foil-bounded section was reached, the burning rate quickly increased along the foil-bonded edge and the acceleration progressed outward until a second steady state emerged—with the burning surface being planar, but no longer making a right angle with the bonded edge. Qualitatively, this course of events was similar to that witnessed with wire-embedded test articles.⁵

Figure 3 illustrates results from a representative test with configuration no. 1. The left image shows deflagration prior to the burning surface reaching the foil. The right image corresponds to a time after the foil had been reached. Data acquired during this test is shown in Fig. 4. It demonstrates the nearly instantaneous transition in burning rate between the 2 sections. The burning rate with respect to the z-axis for the foil-bound section (7.01 cm/s) is almost 390% faster than that measured for the foil-less section (1.44 cm/s).

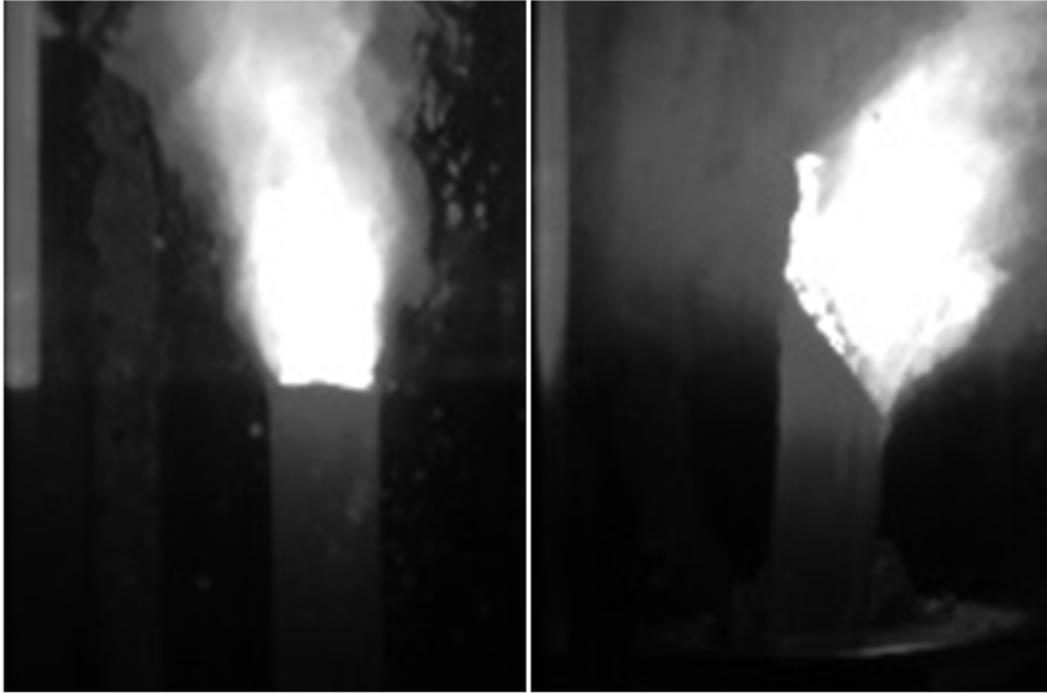


Fig. 2 Results obtained with configuration no. 1 test article: 1) foil-less section (left), 2) section with 0.001-inch-thick Al foil attached to right side (right)

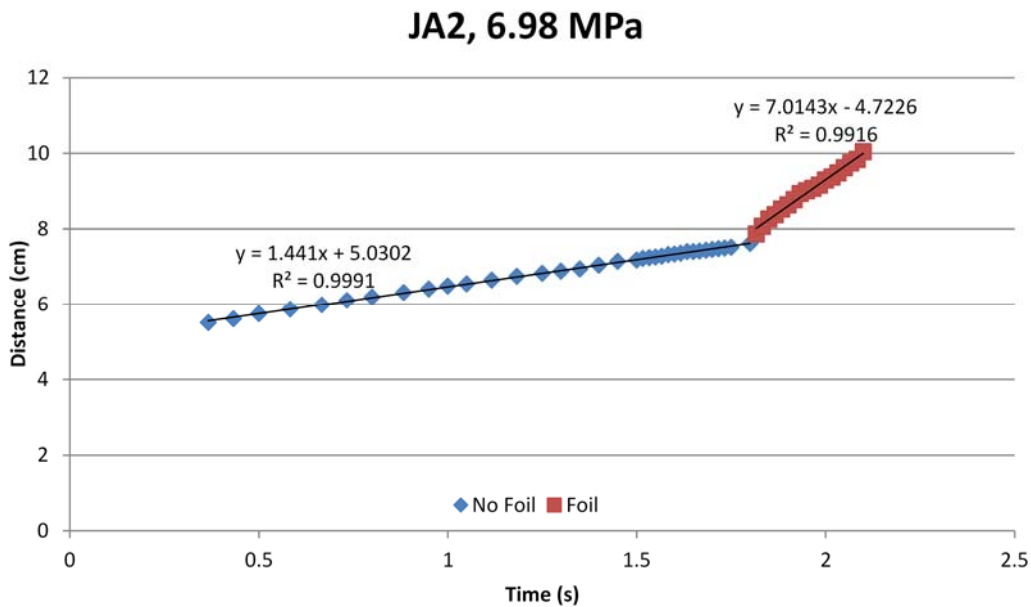


Fig. 3 Data obtained with a configuration no. 1 test article

Table 1 illustrates the wide variability in data recorded. For example, shot 1 experienced a side ignition the instant the foil was reached by the flame so there is no data for the foil section. Others had a noticeable burning rate transition within the foil zone, those are the pressures marked as “a” and “b”, shots 7 and 10 in

particular. Shot 9 appeared to transition between 2 different burning rates within the foil zone. Therefore, a burning rate was calculated for the whole event, and 2 separate burning rates “a” and “b” for the 2 distinct regions.

Table 1 Initial foiled JA2 burning rate data

Test	Foil (Y/N)	P (MPa)	BR (cm/s)	R ²	BR Increase (%)	Θ, Measured (°)	$\sin^{-1}\left(\frac{BR_n}{BR_z}\right)$ (°)
1	N	3.52	0.756	0.9994
2	N	6.96	1.342	0.9988
3	N	6.98	1.441	0.9991
	Y	6.98	7.014	0.9916	387	11.5	11.9
4	Y	6.94	5.496	0.9816	310	15.8	14.1
5	N	5.25	1.047	0.9997
6	Y	5.27a	1.872	0.9946	79	35.7	34
	Y	5.27b	6.858	0.9564	555	13	8.8
7	N	5.30	1.060	0.9990
	Y	5.30a	1.992	0.9905	88	37.6	32.1
	Y	5.30b	5.303	0.9687	400	12.5	11.5
8	N	3.44	0.766	0.9997
	Y	3.44	6.687	0.9655	773	7.3	6.6
9	Y	3.48	2.221	0.9454	190	...	20.2
	Y	3.48a	0.883	0.9765	15	54.6	60.2
	Y	3.48b	1.943	0.9398	154	15.5	23.2
10	N	3.51	0.815	0.9968
	Y	3.51a	2.058	0.9194	153	29	23.3
	Y	3.51b	2.344	0.9842	188	27.5	20.3
11	N	2.02	0.497	0.9988
	Y	2.02	2.221	0.9894	347	18	12.9
12	N	2.03	0.519	0.9986
	Y	2.03	1.535	0.9906	196	14.9	19.8

There were 3 instances where 2 distinct burning rates were observed, a lower early time rate and a significantly higher later time rate. An example of such a result is shown in Fig. 5. From the onset of burning until about 0.45 seconds (s) the burning rate was 1.87 cm/s; however after 0.45 s the burning rate was a much faster 6.86 cm/s. JA2’s baseline burning rate at this pressure is 1.05 cm/s. Therefore, the increase in burning rate was 80% in the beginning but transitioned to a 550% increase towards the end. It is believed that the lack of consistent burning rate increase is due to a foil-propellant bonding issue.

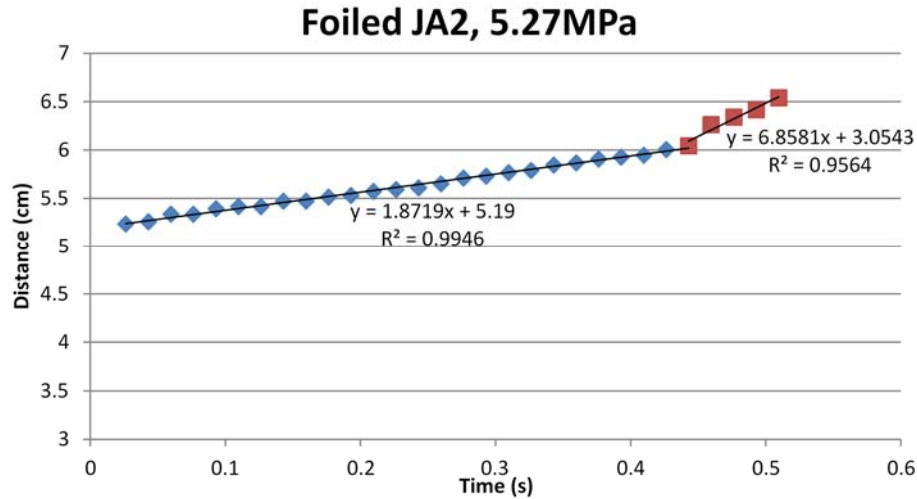


Fig. 4 Bimodal burning rate enhancement of JA2 with foil. (The burning rate of foil-less sections at this pressure were found to be approximately 1.05 cm/s.)

In addition to bimodal behavior, on 2 occasions, there was evidence of side ignition of the propellant in the foil-bound region. Figure 6 shows consecutive images from an experiment where the foil begins to peel off the propellant (inside the red circle) in the first image and in the next image evidence of side ignition is present. The yellow arrows indicate the direction of flame propagation. Again, this phenomenon was likely the result of a bounding issue between the foil and propellant.

However, not all strands burned inconsistently, some strands exhibited a burning behavior like one would expect when compared to a wire-embedded propellant. Thus, some of the data may be useful for modeling purposes.

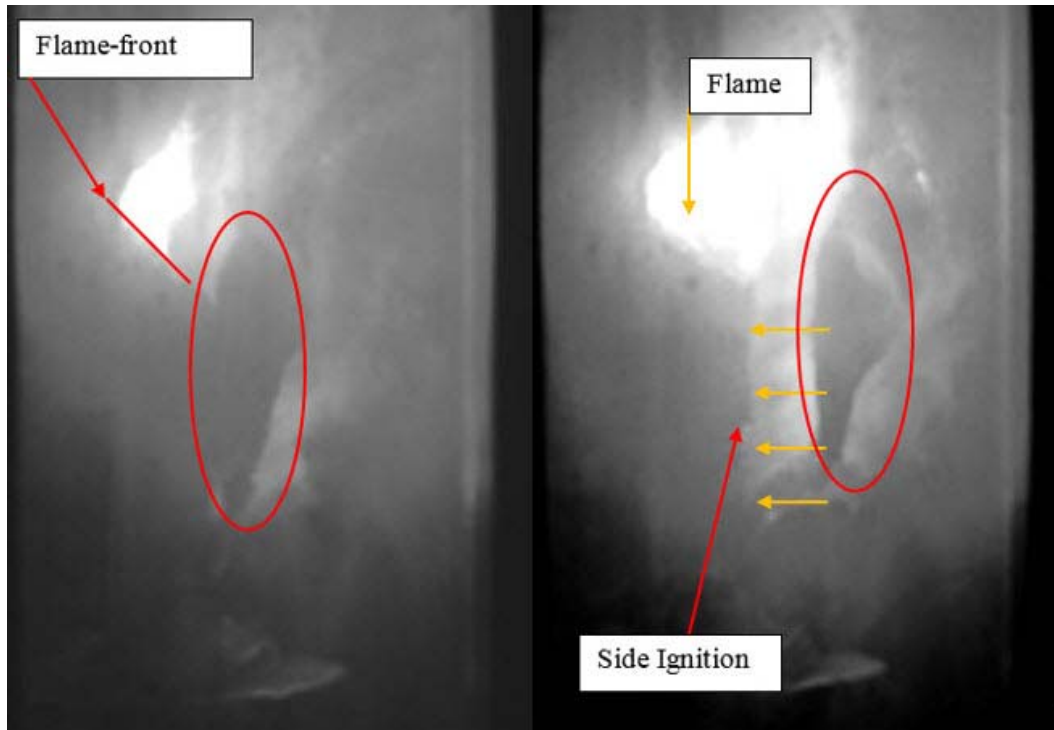


Fig. 5 Consecutive images from JA2 foil experiment at 3.48 MPa. The foil placed on the right side of the propellant for heat transfer purposes is circled. Note the right image has side ignition.

3.2 Configuration No. 2

In configuration no. 2, the total surface area of propellant and aluminum in contact with each other is approximately 0.25 in^2 . This is considerably less than the 1.0 in^2 contact area of configuration no. 1; but still much more than the case of wires, where the greatest surface contact area (associated with the 0.010-inch wire) is approximately $1.57 \times 10^{-4} \text{ in}^2$ surface contact area. For these experiments each strand had a short (approximately 0.3 inch) foil-less section in addition to the foil-bound section (Fig. 7). Figure 8 illustrates a representative profile of the foiled section of propellant.

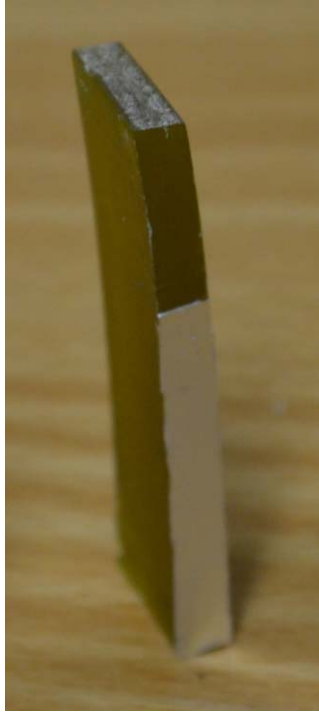


Fig. 6 Test article

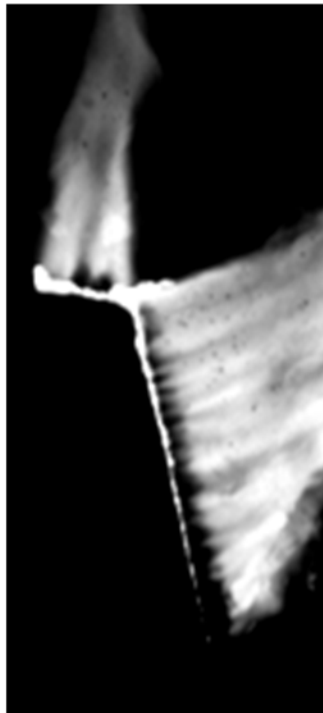


Fig. 7 Image of article burning at 3.52 MPa

At the highest and lowest pressures the measured burning rates were highly reproducible. Results obtained at intermediate pressures were slightly less consistent. Sample 5 had less foil (approximately half the strand) compared to the rest of the samples and exhibited a slower transition to enhanced burning. This could explain why the burning rate measured in this test is significantly lower than the one measured for shot 6. Otherwise, the deflagration exhibited a quick, smooth transition between the foil-less and foil-bound sections. Figures 9 and 10 show the raw burning rate data produced at 6.94 and 2.05 MPa, respectively. Starting times are arbitrary. The raw data for all 8 shots is found in the appendix.

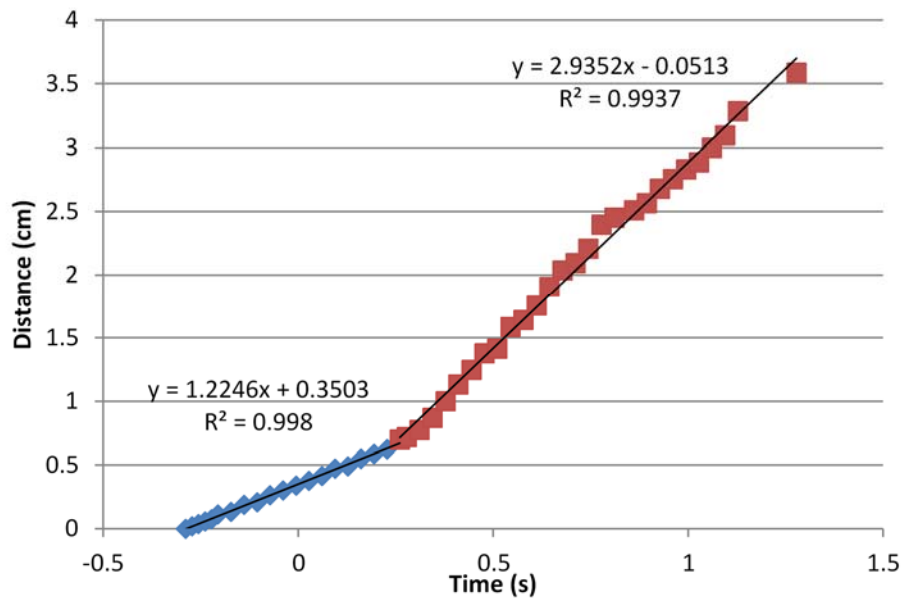


Fig. 8 Test 2, 6.94 MPa burning rate data. Blue is foil-less JA2, red is foil-bounded.

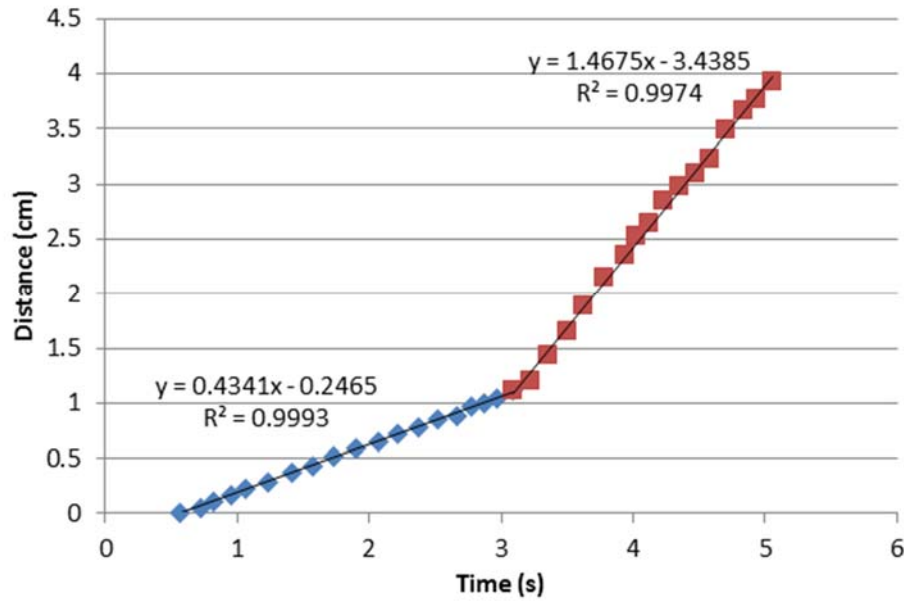


Fig. 9 Test 8, 2.05 MPa burning rate data. Blue is foil-less JA2, red is foil-bounded.

At each pressure, the burning rates measured for the foil-less section were in excellent agreement, and the expression $0.245 \cdot P^{0.804}$ fit the data with a coefficient of determination of 0.993. Table 2 also includes the mass flux rates measured for each test. They were calculated by multiplying the burning rate measured with respect to the z-axis by the density of JA2 (1.60 g/cc).

Table 2 Foiled JA2 burning rate data

Test	P (MPa)	Foil	BR _z ^a (cm/s)	Mass Flux (g/cm ² -s)	% Increase	Θ, measured (°)	Θ, $\sin^{-1} \left(\frac{BR_n}{BR_z} \right)$ (°)
1	6.94	No	1.175	1.88
	6.94	Yes	3.154	5.05	168	20.6	21.9
2	6.94	No	1.225	1.96
	6.94	Yes	2.935	4.70	140	22.9	24.7
3	5.23	No	0.893	1.43
	5.23	Yes	3.541	5.67	297	15.5	14.6
4	5.23	No	0.874	1.40
	5.23	Yes	2.556	4.09	193	21.2	20.0
5	3.49	No	0.674	1.08
	3.49	Yes	1.664	2.66	147	25.7	23.9
6	3.52	No	0.674	1.08
	3.52	Yes	2.796	4.47	315	14.2	13.9
7	2.05	No	0.443	0.71
	2.05	Yes	1.532	2.45	246	17.7	16.8
8	2.05	No	0.434	0.69
	2.05	Yes	1.467	2.35	238	17.0	17.2

^aBurning rate with respect to the z-axis.

For the foiled propellant, gas generation rate increases ranged from 150% to 300% with the amount of increase greatest at the lower pressures. Data analysis shows that the average burning rate increase at 2.05, 3.50, and 5.23 MPa to be 242%, 230%, and 245%, respectively. This suggests that there is a finite burning rate increase possible with the presence of a thermally conductive foil and that we have reached that maximum. Also, in contrast to wire-embedded strands, the foil-bounded strands did not show burning rate increases less than 100%. Embedded with thin wires, burning rate increases between 20% and 50% were observed at low pressures.

Figure 11 plots the data of Table 2 and shows the flatter burning rate increase with respect to pressure of the foil-bounded propellant. The lower burning rate exponent indicates that the foiled propellant's performance is less dependent on pressure; however, there is still a burning rate dependence on pressure (i.e., higher burning rates at higher pressures). A statistical analysis of these limited data shows that they are not sufficient to prove that they are different. At a 90% confidence interval, the burning rate exponent of the foiled propellant ranges from 0.22 to 0.90. At the same confidence, the foil-less burning rate exponent ranges from 0.75 to 0.94. It should be noted that this observation is only valid for the relatively low-pressure regime at which the experiments were conducted, maximum 6.93 MPa (1,000 psi).

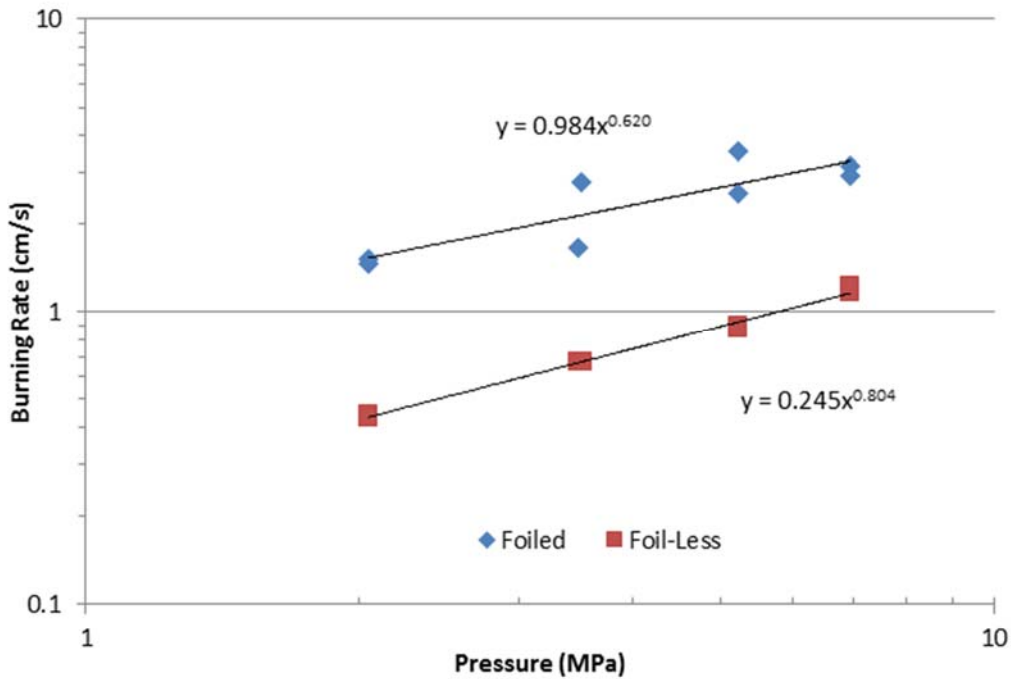


Fig. 10 Summary of burning rate vs. pressure for neat and foiled JA2

Table 2 and Fig. 12 also shows measured surface-foil angles (Θ) and compares them to the angle calculated based on the foil-less linear burning rate of JA2 and the (enhanced) burning rate measured with respect to the z-axis (BR_z). If the burning rate normal to the surface (BR_n) is the same as the normal linear burning rate, then based on geometric considerations,

$$\cos(90 - \Theta) = \left(\frac{BR_n}{BR_z} \right) \quad (1)$$

or

$$\Theta = \sin^{-1} \left(\frac{BR_n}{BR_z} \right) . \quad (2)$$

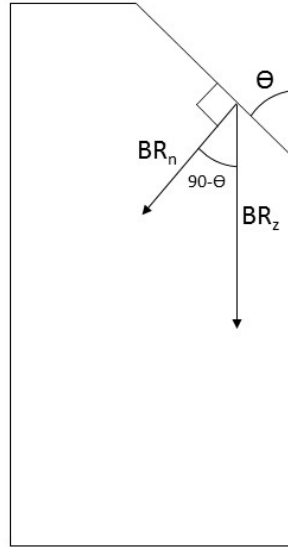


Fig. 11 Diagram of deflagration profile

As such, the results indicate that other phenomena that might increase the normal linear burning rate, such as in-depth heating of the bulk propellant or erosive burning due to convective flows directed across the burning surface, play little if any role. Rather, the foil acts primarily as an ignition source that serves to propagate a deflagration normal to the side wall, increasing the area of the burning surface.

Results from these experiments will be transitioned to the ARL's modeling effort with the goal of being able to accurately predict enhanced mass generation rates and surface topology for nitrate-ester based propellants embedded with thermally conductive materials, whether the material is a foil or wire. Ideally, actual wire-embedded rocket propellant would be burned in the strand burner to determine application-related enhanced burning rate characteristics. However, we do not have an in-house capability for making them. Thus they need to be furnished by a third party.

3.3 Other Observations

The videographs clearly show that JA2 burning in this pressure regime has cellular structure, particularly at the foil-propellant interface. This cellular structure was present and stable throughout the burning event. Figure 13 shows this quite well as the dark zone of the flame forms many small arches above the propellant surface.

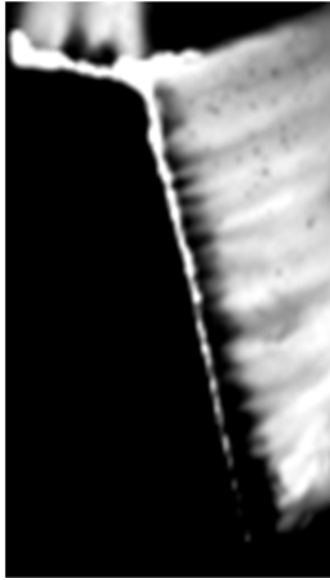


Fig. 12 Close-up of burning surface illustrating cellular flame structure

Finally, 1 variable in the experimental setup that was not considered in the analysis of the results is the flow rate of nitrogen gas over the strands as they were being burned. The gas was flowed from the base of the propellant strand toward the exhaust located at the top of the chamber to clear any smoke that might have obscured the video imaging. The gas flow rate was controlled by 2 hand-turned valves, 1 for the inlet and 1 for exhaust. Adjusted together to maintain constant pressure inside the chamber and with the intent to keep it at a minimum, it is nevertheless quite likely that flow rate varied from test to test. Introducing this flow may ultimately introduce a cooling effect on the strand, which could alter heat transfer rates through the metal foil and produce inconsistent results.

4. Summary and Conclusions

Experiments were conducted to visualize the deflagration of foil-bounded JA2 strands at pressures from 2 to 7 MPa. Normal linear burning rates, burning rates relative to the strand's side wall, and angles between the surface and the sidewall were measured. Considered together, the results indicate that the increase in gas (mass) generation rates observed, which ranged from 150% to 250%, were primarily due to the foils acting as an ignition source that served to propagate a

deflagration wave normal to the side wall, increasing the total area of the burning surface. Other phenomena that might increase the rate, such as in-depth heating of the bulk propellant or erosive burning due to convective flows directed across the burning surface, appear to play little if any role. It was also observed that the gas generation rate for foil-bounded strands was less pressure dependent than that for the baseline (foil-less) configuration. Finally, the videographs showed that although the surface regressed in a steady, planar manner, the gas-phase flame has cellular structure. Pertaining to a relatively simple geometry, these results should provide a good basis with which to validate CFD models for simulating the deflagration of wire-embedded propellants.

5. References

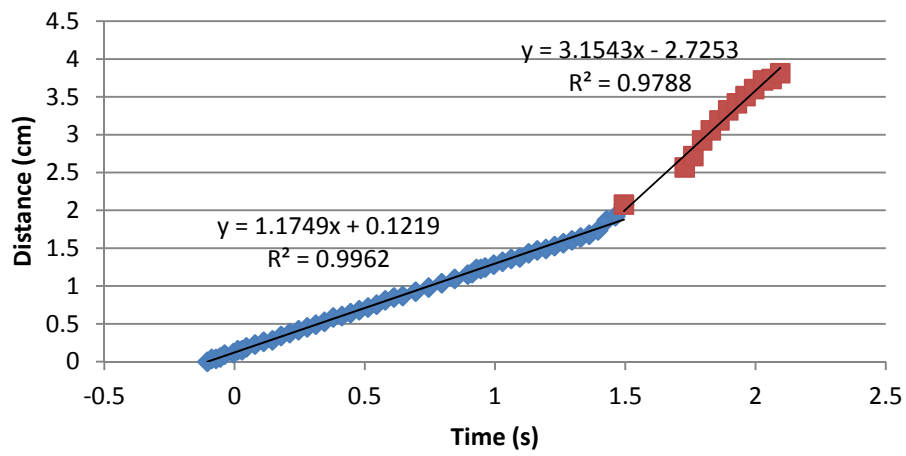
1. Kubota N, Ichida M. Combustion processes of propellants with embedded metal wires. *AIAA Journal*. Jan 1982;20(1):AIAA 31–1207R.
2. King MK. Analytical modeling of effects of wires on solid motor ballistics. *Journal of Propulsion*. May–June 1991;7(3).
3. Graham PH. Studies of wire end-burning propellant. Atlantic Research Corporation; 1974 Nov. Report No.: AFRPL-TR-74-85.
4. Childs LB Jr, Cockrell BL, Graham PH, Sullivan E, Jennings JD. High rate technology improvements. Atlantic Research Corporation; 1978 Oct. Report No.: TR-T-CR-79-12.
5. Ritter J, Wingard Z, Canami A, McBain A. Visualization and measurement of the burning surface of wire-embedded energetic materials, Part I: JA2 and Pentolite. Aberdeen Proving Ground (MD): Army Research Laboratory (US); 2014 June. Report No.: ARL-TR-6959.
6. Shuling C, Fengsheng L. Influence of Long Metal Wires on Combustion of Double-Base Propellants. *Combustion and Flame*. 1982;45:213–218.
7. Rumbel KE, Cohen M, Henderson CB, and Scurlock AC . A physical means of attaining high burning rate in solid propellants. Paper presented at: the Eleventh Joint Army-Navy-Air Force Solid Propellant Meeting; 1955 May; Washington.
8. Nusca MJ, Gough PS. Numerical model of multiphase flows applied to solid propellant combustion in gun systems. Paper No. AIAA 1998-3695 presented at: Proceedings of the 34th AIAA/ASME/SAE/ASEE Joint Propulsion Conference and Exhibit; 1998 July; Cleveland, (OH).
9. Nusca MJ. Modeling the burning rate of solid propellants with embedded metal wires. Proceedings of the 38th JANNAF Propellant and Explosives Development and Characterization Meeting; 2014 May; Charleston (SC).
10. Miller M, Anderson W. Burning-rate predictor for multi-ingredient propellants: nitrate-ester propellants. *Journal of Propulsion and Power*. 20:440–454.
11. Anderson W, Meagher N, Vanderhoff J. Dark zones of solid propellant flames: critical assessment and quantitative modeling of experimental datasets with analysis of chemical pathways and sensitivities. 2011 January. Aberdeen Proving Ground (MD): Army Research Laboratory (US); Report No.: ARL-TR-5424.
12. Miller M, Vanderhoff J. Burning Phenomena of Solid Propellants. Aberdeen Proving Ground (MD): Army Research Laboratory (US); 2001 July. Report No.: ARL-TR-2551.

Appendix. Raw Data

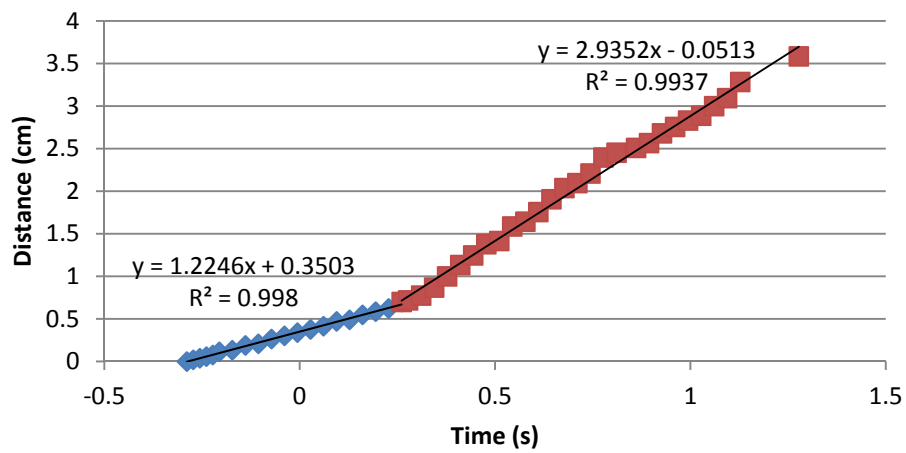
This appendix appears in its original form, without editorial change.

Foil on 0.150-in surface (Fig. 1c). Blue is foil-less JA2 and red is foiled section of JA2.

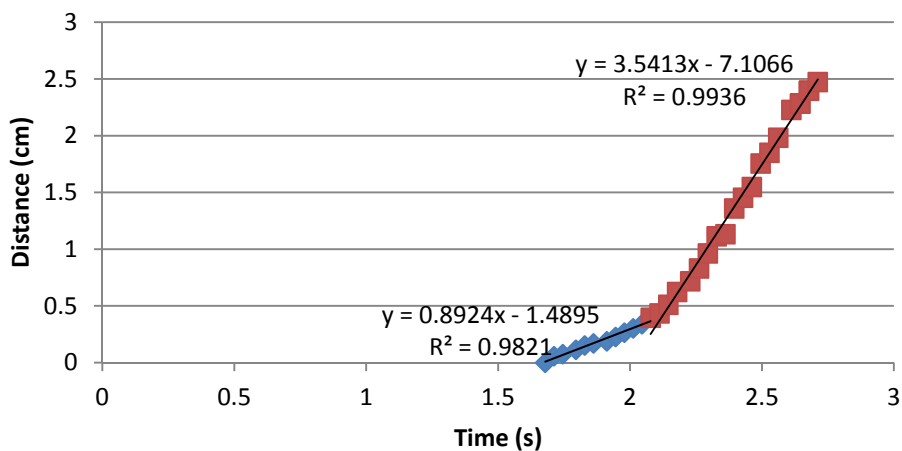
Sample 1, 6.94 MPa



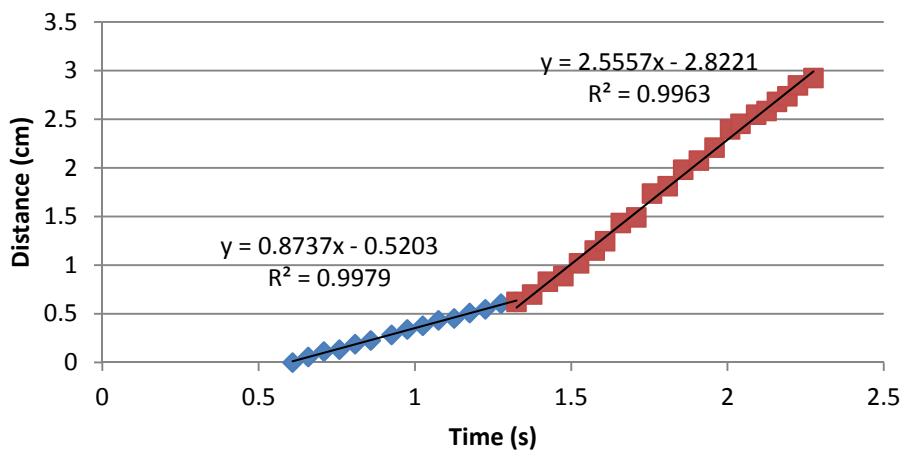
Sample 2, 6.94 MPa



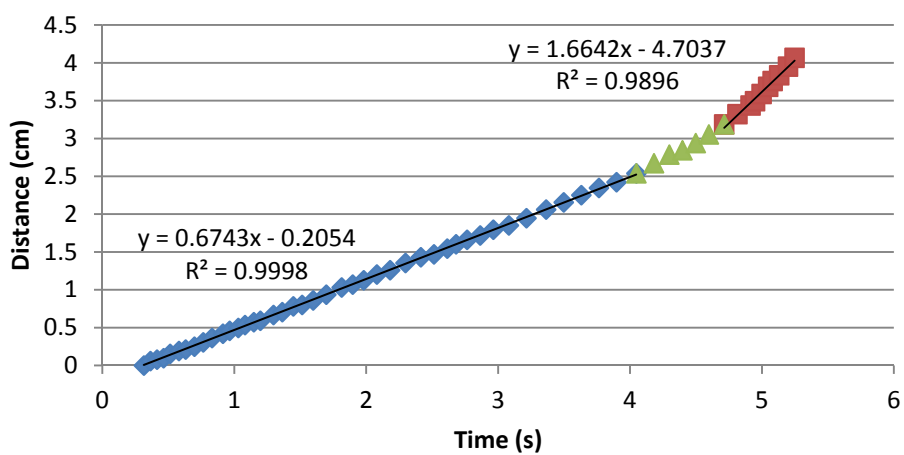
Sample 3, 5.23 MPa



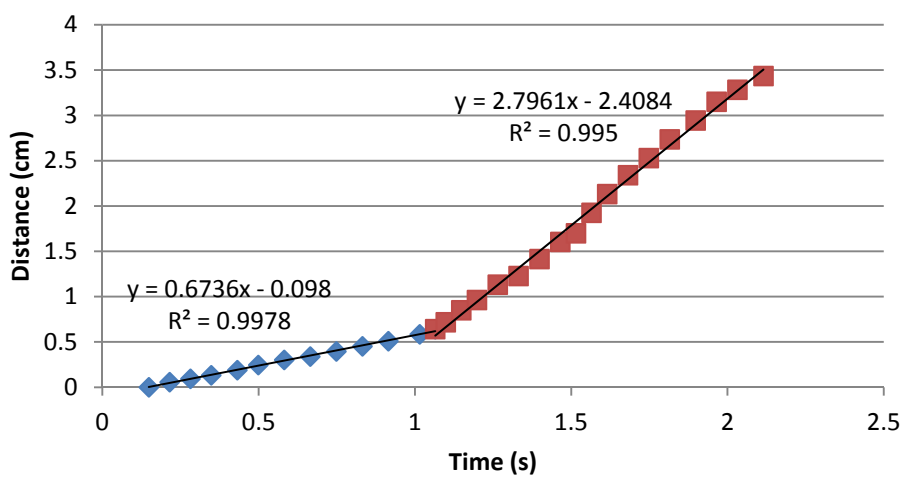
Sample 4, 5.23 MPa



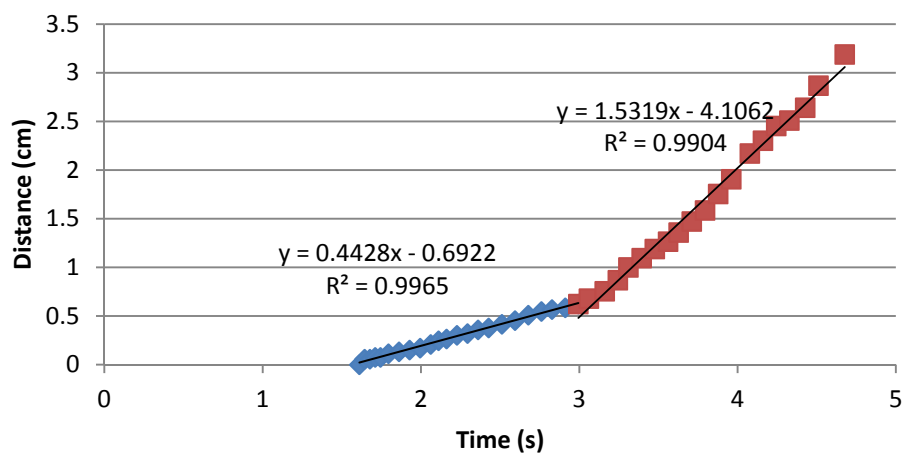
Sample 5, 3.49 MPa



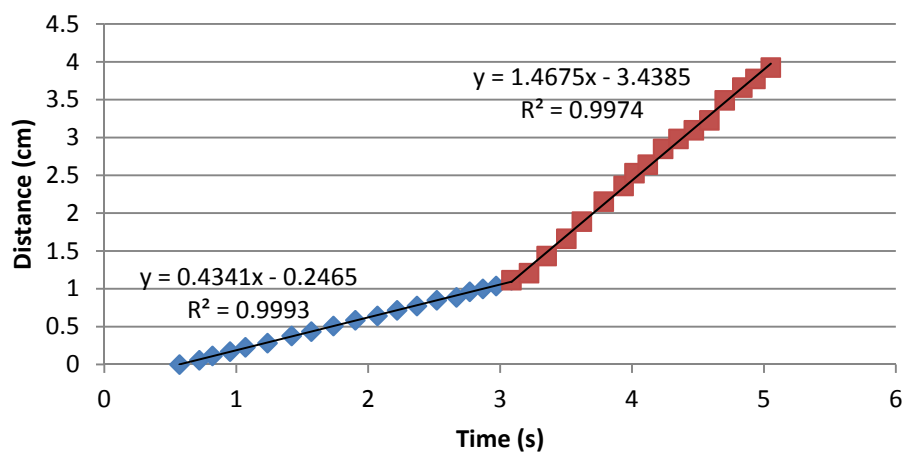
Sample 6, 3.52 MPa



Sample 7, 2.05 MPa



Sample 8, 2.05 MPa



INTENTIONALLY LEFT BLANK.

List of Symbols, Abbreviations, and Acronyms

θ	theta; cone angle of flame
AMRDEC	US Army Missile Research, Development, and Engineering Center
ARL	US Army Research Laboratory
BR	Burning Rate
cc	cubic centimeters
CFD	computational fluid dynamics
cm	centimeter
cm/s	centimeter per second
DEGDN	diethylene glycol dinitrate
fps	frames per second
in ²	square inches
P	Pressure
psi	pounds per square inch
MPa	Mega Pascal
mm	millimeter
NC	nitrocellulose
NG	nitroglycerin
R ²	coefficient of determination
s	second(s)
μ s	microsecond

1 DEFENSE TECHNICAL
(PDF) INFORMATION CTR
DTIC OCA

2 DIRECTOR
(PDF) US ARMY RESEARCH LAB
RDRL CIO LL
IMAL HRA MAIL & RECORDS
MGMT

1 GOVT PRINTG OFC
(PDF) A MALHOTRA

1 COMMANDER
(PDF) US ARMY ARDEC
RDAR MEE W
K KLINGAMAN

1 COMMANDER
(PDF) US ARMY ARDEC
RDAR MEE P
J WYCKOFF

3 COMMANDER
(PDF) US ARMY ARDEC
RDAR MEE W
E CARAVACA
L LOPEZ
M KAUFFMAN

4 COMMANDER
(PDF) US ARMY AMRDEC
RDMR WDP P
A GERARDS
P HABERLEN
J NEIDERT
D THOMPSON

6 COMMANDER
(PDF) US ARMY AMRDEC
RDMR WDP E
C DOLBEER
G DRAKE
A DURRETT
M KIRKHAM
L PLEDGER
N MATTHIS

1 PENN STATE UNIVERSITY
(PDF) S THYNELL

3 PURDUE UNIVERSITY
(PDF) A MCBAIN
D REESE
S SON

ABERDEEN PROVING GROUND

30 DIR USARL
(PDF) RDRL WM
S KARNA
B FORCH
RDRL WML
M ZOLTOSKI
RDRL WML A
W OBERLE
RDRL WML B
N TRIVEDI
RDRL WML C
S AUBERT
RDRL WML D
R BEYER
A BRANT
C CHEN
J COLBURN
P CONROY
T DUTTON
S HOWARD
M MCQUAID
M NUSCA
J RITTER
J SCHMIDT
J VEALS
A WILLIAMS
Z WINGARD
RDRL WML E
P WEINACHT
RDRL WML F
M ILG
RDRL WML G
J SOUTH
T BROSSEAU
A MICHLIN
RDRL WML H
J NEWILL
T EHLERS
T FARRAND
L MAGNESS
RDRL WML C
P KASTE